Pergamon

Bioorganic & Medicinal Chemistry 10 (2002) 2751–2757

BIOORGANIC & MEDICINAL CHEMISTRY

Effect of Protonation of the *N*-Acetyl Neuraminic Acid Residue of Sialyl Lewis^X: A Molecular Orbital Study with Insights into Its Binding Properties toward the Carbohydrate Recognition Domain of E-Selectin

Fabio Pichierri* and Yo Matsuo

Computational Proteomics Team, Bioinformatics Group, RIKEN Genomic Sciences Center, 1-7-22 Suehiro-cho, Tsurumi-ku, Yokohama 230-0045, Japan

Received 1 October 2001; accepted 1 February 2002

Abstract—Semiempirical molecular orbital (MO) calculations with an implicit treatment of the water environment were employed in order to assess whether the sialyl Lewis^X (sLe^X) tetrasaccharide binds to E-selectin in the anionic or neutral (i.e., protonated) state. The analysis of the frontier molecular orbitals, electrostatic potential surfaces, and conformational behavior of the sugar indicates that its neutral form possesses the necessary characteristics for binding. In particular, the LUMO level of the neutral sLe^X molecule is localized both on the carboxylic group of the *N*-acetyl neuraminic acid (NeuNAc) residue and on the nearby glycosidic linkage. These two moieties interact with the Arg97 residue of E-selectin, as revealed by a recent crystal structure analysis of the E-selectin/sLe^X complex. The energetics of this specific interaction was investigated with the aid of ab initio Hartree–Fock MO calculations, which resulted in a BSSE-corrected binding energy of 16.63 kcal/mol. Our observations could open up new perspectives in the design of sLe^X mimics.

Introduction

The sialyl Lewis^X (sLe^X) tetrasaccharide, αNeuNAc(2-3)βGal(1-4)[αFuc(1-3)]βGlcNAc), whose chemical structure is depicted in Figure 1, is the target epitope recognized by selectins.[1–3] The latter are membrane proteins that are able to weakly bind the sLe^X moiety via their carbohydrate recognition domains (CRDs).[4] As a result of post-translational modifications, the sLe^X epitope is found in glycoproteins that are located on the surfaces of white blood cells (i.e., leukocytes). This allows leukocyte adhesion onto endothelial cells to occur thereby initiating the inflammatory reaction when tissue injury takes place.[3]

Somers et al.[5] have recently determined the crystal structures of both E- and P-selectin in complex with sLe^X. They have also determined the structure of P-selectin in complex with SGP-3, a sulphated glycopeptide with high binding affinity for the CRDs of selectins. The three-dimensional (3-D) structures of the first two protein/ligand complexes are of particular interest since they show, for the first time, important details about the binding mode between the CRDs of selectins and sLe^X. Although the sugar in the bioactive conformation interacts with either selectin in a very similar fashion, higher affinity has been ascribed to the E-selectin/sLe^X complex.[5] In the latter, both the galactosyl (Gal) and *N*-acetyl neuraminic acid (NeuNAc) moieties of the tetrasaccharide are engaged in five atom-atom contacts with four amino acid residues located on the protein CRD, namely Tyr48, Glu92, Tyr94, and Arg97, respectively. In particular, the Arg97 residue interacts with both the oxygen atom of the αNeuNAc(2-3)βGal glycosidic linkage and the carboxylic group of the NeuNAc moiety (see Fig. 1). The latter group interacts also with the Tyr48 residue to form an additional (Tyr48)OH···O=C hydrogen bond. Figure 2 shows the spatial orientation of these two residues on the CRD of E-selectin, which has been structurally characterized by Graves et al. (PDB code: 1ESL).[6] The CRDs of both selectins possess a surface-bound Ca^{2+} ion that engages the 3- and 4-hydroxyl groups on the fucosyl (Fuc) moiety of sLe^X (see Fig. 1) through ion-dipole interactions. Additional contacts, involving

*Corresponding author. Tel.: +81-45-507-2523; fax: +81-45-507-2524; e-mail: fabio@gsc.riken.go.jp

0968-0896/02/$ - see front matter
PII: S0968-0896(02)00092-5

also the 2-hydroxyl group, are established with Glu80, Asn82, and Asn105, along with a water molecule, respectively.[5]

The carboxylic group born by the NeuNAc residue is a key element of the sLe^X epitope and its deletion represents one of the most straightforward substitutions thus far exploited by medicinal chemists[3] in designing sLe^X mimics. Earlier models[3] have suggested that, if negatively charged, the carboxylate group would interact with the positively charged amide groups of Arg97, to yield the salt bridge shown in Figure 3a. However, the 3-D structure of the E-selectin/sLe^X complex recently determined by Somers et al.[5] clearly shows the carboxylic group of NeuNAc interacting with the NH moiety of the Arg97 residue, as shown in Figure 3b. This novel experimental result suggests that the sugar is likely to interact with E-selectin in the neutral (i.e., protonated) rather than in the anionic state. Knowledge of the ionic state of the bounded sugar might be useful in designing new sLe^X mimics in which a neutral chemical group replaces the carboxylic moiety on NeuNAc. Unfortunately, owing to the intrinsic limitations of protein X-ray crystallography in locating hydrogen atoms,[7] the experimental structures of the protein/sugar complexes characterized so far cannot reveal whether the bound tetrasaccharide is protonated or not. This information, however, could be supplied by molecular modeling.

In the present article we will investigate the effect of protonation on the structural, conformational, and electronic properties of sLe^X by means of semiempirical molecular orbital (MO) calculations.[8] The latter allow one to treat large molecules, that is containing a hundred or more atoms, at a quantum mechanical level.[9–11] Furthermore, the effects of the aqueous environment can be efficiently included during geometry optimization by means of implicit solvation models.[12] Hence, this computational approach represents an attractive alternative to molecular mechanics methods in that it avoids a painstaking parameterization of the force field.[13]

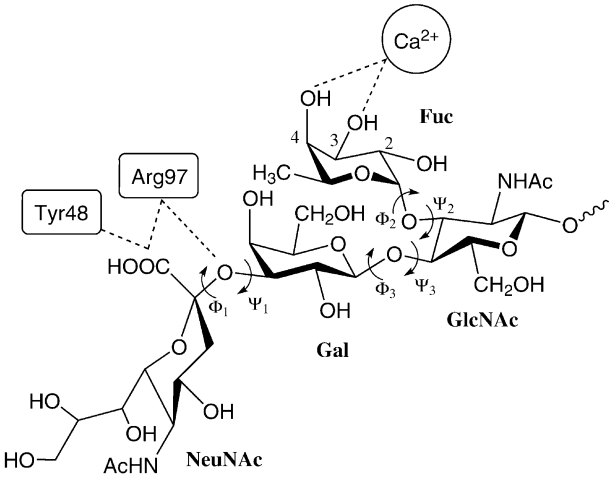

Figure 1. Chemical structure of the sLe^X epitope. The carboxylic group on NeuNAc interacts with both the Arg97 and Tyr48 residues of E-selectin. The Fuc moiety interacts with a protein-bound Ca^{2+} ion through its 3- and 4-hydroxyl groups. Additional interactions are described in the text.

Results

We started our computations by employing the experimental structure of one bioactive conformer (**A1**) of sLe^X, which has been determined in complex with a mutant of the rat serum mannose binding protein (MBP; PDB code: 2KMB).[14] This choice was dictated by the fact that, at the time the present study was undertaken, the atomic coordinates of both E-selectin/sLe^X and P-selectin/sLe^X complexes recently determined by Somers et al.[5] were not available in the PDB.[15]

The Fuc moiety of the sLe^X molecule in complex with MBP employs its 2- and 3-hydroxyl groups in order to coordinate the protein-bound Ca^{2+} ion.[14] Also, other interactions that have been observed in both E- and P-selectin complexes are absent here. Nevertheless, the experimental structure of this bioactive conformer (**A1**) represents a good starting point for modeling the family of conformers labeled **A**. According to the conformational data recently reviewed by Imberty and Péres,[16] in this family ϕ_1 ranges from 41 to 77° while ψ_1 ranges

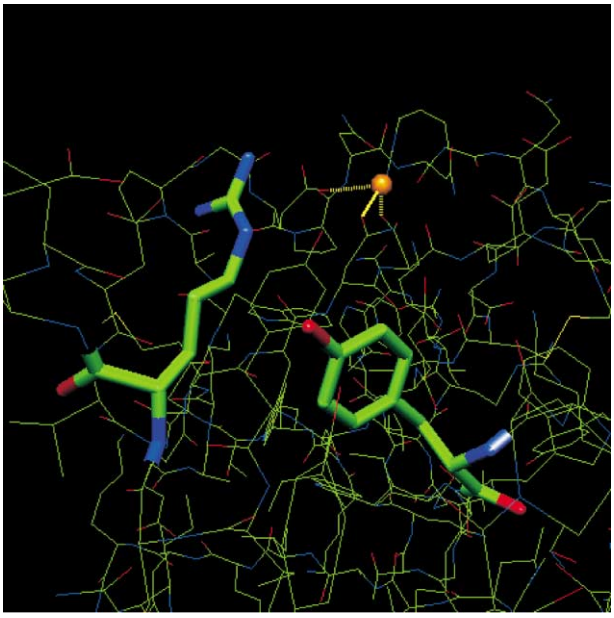

Figure 2. Spatial arrangement of the Arg97 and Tyr48 residues on the CRD of E-selectin; the protein bound Ca^{2+} ion is represented by a yellow ball. This image was produced with our graphics software Tornado.

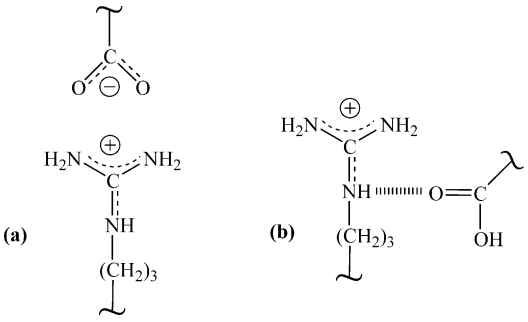

Figure 3. Comparison between (a) an earlier prediction and (b) the experimentally observed interaction mode between the carboxylic group of sLe^X and the Arg97 residue of E-selectin.

from 82 to 130°. Two other families of low-energy conformers of sLe^X, labeled **B** and **C**, respectively, have been identified. The latter two families differ from **A** in the orientation of the NeuNAc moiety (Fig. 1) about the αNeuNAc(2-3)βGal glycosidic linkage, whereas the remaining portion of the sugar appears to be relatively stereo-rigid.[16] In family **B**, ϕ_1 ranges from −40 to −57° (a lower bound of −22° has also been obtained by molecular dynamics simulation[17]) and ψ_1 ranges from 93 to 116°. In family **C**, ϕ_1 ranges from −172 to −178° and ψ_1 ranges from 100 to 108°. It is worth noticing that conformer **B** was the first to be identified by NMR spectroscopy (see ref. 16 for a detailed account) and, hence, is likely to be the most populated in solution.

Table 1 reports the converged heats of formation (HOF), dipole moments and HOMO–LUMO gaps of the three canonical low-energy conformers (**A**, **B**, **C**) of sLe^X in both the neutral and anionic states, as calculated with both the AM1/COSMO (ε = 78.5) and PM3/COSMO (ε = 78.5) methods. The corresponding optimized torsion angles are given in Table 2, together with those of three experimentally determined **A**-type structures (**A1**, **A2**, and **A3**)[14] reported at the bottom three rows of Table 2.

The optimized AM1 values of ϕ_i and ψ_i (with $i = 1$–3) for conformer **A** in the anionic form correspond to 53 and 98° ($i = 1$), −70 and 142° ($i = 2$), and −81 and −97° ($i = 3$), respectively. As for the PM3 values, all the torsion angles but ϕ_1 (66°) are very close to those calculated with the AM1 method. Protonation of the carboxylic group on NeuNAc, to yield the neutral tetrasaccharide, provokes only a slight change of ϕ_1, which decreases from 53 to 46° (AM1/COSMO). The corresponding change of ϕ_1 calculated with the PM3/COSMO method amounts to ∼10°. Overall, the structures of conformer **A** optimized with both semiempirical MO methods are in good agreement with the experimental one, especially when the comparison is done against both the **A1** and **A3** structures.

Setting the torsion angles at values in the above ranges optimized conformers **B** and **C**, respectively. Inspection of the optimized torsional parameters ϕ_1 and ψ_1 reported in Table 2 indicates that the AM1/COSMO values calculated for **B**, either in the anionic or neutral state, are well within the above literature ranges.[16] On the other hand, the corresponding PM3/COSMO values are slightly out of range for both the anionic and neutral states. As for conformer **C**, only the AM1 value of ψ_1 appears to be slightly larger than those expected for both states, whereas the calculated PM3 values of both ϕ_1 and ψ_1 are out of range for either state. Overall, the AM1/COSMO method appears to perform better than PM3/COSMO in reproducing the geometries of both **B**

Table 1. Heats of formation (HOF, in kcal/mol), dipole moments (in Debye) and HOMO–LUMO energy gaps (in eV) of the anionic and neutral forms of the canonical sLe^X conformers as calculated with the AM1/COSMO and PM3/COSMO methods

Form	Conformer	AM1/COSMO			PM3/COSMO		
		HOF	Dipole	HOMO–LUMO	HOF	Dipole	HOMO–LUMO
Anion	**A**	−1257.969619	30.4	11.00	−1173.503234	31.7	10.51
	B	−1275.012660	27.2	11.03	−1181.248118	27.2	10.49
	C	−1272.620807	23.2	10.94	−1185.747942	27.0	10.48
Neutral	**A**	−1161.094987	8.3	10.27	−1061.208989	7.4	9.92
	B	−1173.455732	9.9	10.40	−1075.998612	10.4	10.09
	C	−1171.100163	16.5	10.38	−1077.412626	16.3	10.11

Table 2. Torsion angles of the canonical conformers of the sLe^X tetrasaccharide in the anionic and neutral forms as calculated with the AM1/COSMO and PM3/COSMO methods

Form	Method	Conformer[a]	αNeuNAc(2-3)Gal		αFuc(1-3)GlcNAc		βGal(1-4)GlcNAc	
			Φ_1	Ψ_1	Φ_2	Ψ_2	Φ_3	Ψ_3
Anion	AM1/COSMO	**A**	53	98	−70	142	−81	−97
		B	−55	114	−82	143	−82	−97
		C	−175	116	−77	143	−82	−99
	PM3/COSMO	**A**	66	97	−73	144	−93	−96
		B	−63	118	−82	142	−86	−94
		C	−163	93	−74	143	−90	−100
Neutral	AM1/COSMO	**A**	46	102	−72	144	−79	−98
		B	−53	110	−78	142	−81	−98
		C	−175	114	−77	143	−83	−98
	PM3/COSMO	**A**	56	100	−70	145	−92	−87
		B	−65	117	−82	142	−87	−93
		C	−156	96	−79	142	−87	−94
Experimental[b]		**A1**	50	94	−68	133	−87	−95
		A2	68	82	−70	85	−72	−97
		A3	51	101	−70	140	−75	−109

[a]See Figure 1 for the corresponding torsion angles. The convention adopted here is the same as that of ref. 16 where Φ = O6–C2–O2–C3′ and Ψ = C2–O2–C3′–C4′.
[b]Experimental data taken from ref. 14.

and **C**. Furthermore, the higher stability calculated for **B** (Table 1) in either state agrees with the fact that, being the first conformer detected by NMR spectroscopy,[16] it is likely to be the most populated in solution. Hence, we will limit our further discussion to the AM1/COSMO results only.

Discussion

Dipole moments

As reported in Table 1, the magnitude of the calculated (AM1/COSMO) dipole moment of the anion ranges from 30.4 Debye (**A**) to 27.2 Debye (**B**) and 23.2 Debye (**C**), respectively. Protonation of the carboxylic group of the NeuNAc residue decreases the magnitude of the total dipole moment by about 2–3 times. It is useful to determine the relative orientation of the dipole moment vector of sLe^X with respect to its binding site on the CRD.

Figure 4 compares the dipole moment vectors calculated for the anionic and neutral forms of the bioactive conformer **A**, respectively. In each state, the origin of the dipole moment vector is located at the middle point of the C1–C2 bond of the central Gal residue. Both vectors are approximately oriented toward the GlcNAc residue. With respect to the binding site on the CRD of E-selectin, we notice that the dipole moment vectors do not point toward the protein-bound Ca^{2+} ion (indicated by an asterisk). The latter interacts with both the 3- and 4-hydroxyl groups of Fuc (Fig. 1) and is coordinated to Asn83, Asp106, Asn82, and Asn105 residues on the CRD.[5,6] This result suggests that a possible role of the metal ion might be that of increasing the strength of the protein/ligand interaction rather than that of favoring the correct orientation of the sugar on the CRD. Care, however, should be exercised in interpreting the results based only on the ligand's dipole moment.[18] Macrodipoles of up to about 1500 Debye are typical for protein molecules and are expected to add up to millions of Debye when the protein is embedded within the cell membrane.[19] An estimate of the permanent dipole moment of E-selectin is, however, out of the scope of the present study.

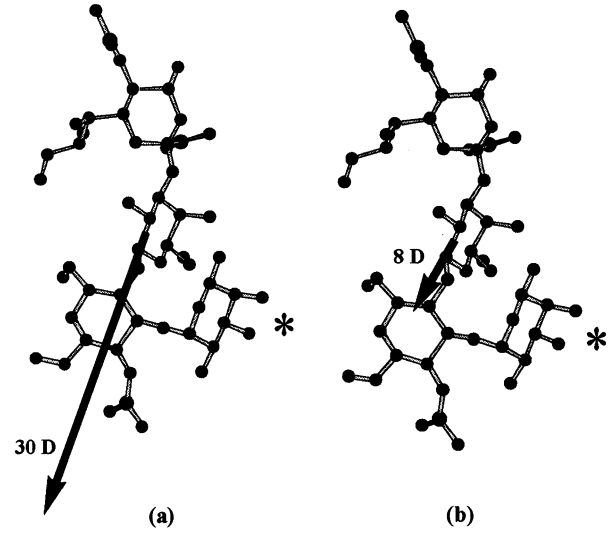

Figure 4. Comparison between the calculated dipole moment vectors of the sLe^x molecule (conformer **A**) in the (a) anionic and (b) neutral state. In each drawing, the NeuNAc residue is on the top and the GalNAc residue on the bottom. The protein-bound Ca^{2+} ion is depicted with an asterisk. Hydrogen atoms have been omitted for clarity.

Frontier orbitals

Table 1 reports also the HOMO–LUMO energy gaps calculated for each sLe^X conformer herein investigated. It appears that protonation of the NeuNAc residue decreases the HOMO–LUMO energy gap in each conformer by about 0.7 eV (AM1/COSMO results). This change might adjust the energy of the frontier orbitals of sLe^X relatively to those of the protein thereby favoring the occurrence of specific intermolecular interactions. To assess further the role played by orbital interactions[20,21] in receptor/ligand binding, it is worth analyzing in more detail the topology of the frontier MOs of sLe^X. Figure 5 reports the 3-D contour plots of the frontier MOs of the bioactive conformer **A** in both its anionic and neutral states. In the anion, the HOMO, shown in Figure 5a, is localized on the NeuNAc residue while the LUMO, shown in Figure 5b, is localized on the peptide bond moiety of GlcNAc. In the neutral tetrasaccharide, the HOMO, shown in Figure 5c, is also localized on the NeuNAc residue but the LUMO, shown in Figure 5d, is localized exclusively on both the carboxylic group of NeuNAc and the glycosidic oxygen connecting NeuNAc to Gal (Fig. 1).

Interestingly, the latter two moieties are H-bonded to the Arg97 residue of E-selectin, as revealed by the recent crystal structure analysis of Somers et al.[5] and schematically depicted in Figures 1 and 3b. This result suggests that the frontier MOs of the neutral sLe^X molecule are likely to interact with protein MOs localized on the CRD. We will check the truthfulness of this prediction by means of linear-scaling semiempirical calculations,[9] as soon as the atomic coordinates of the E-selectin/sLe^X complex will be available in the PDB.

NeuNAc/Arg97 interaction

In order to quantify the strength of the NeuNAc/Arg97 interaction, we have performed ab initio MO calculations on a H-bonded dimer model containing the positively charged terminal fragment of Arg97 and the protonated carboxylic group of NeuNAc. The structure of the title supermolecule, optimized at the HF/6-31G(d,p) level of theory, is shown in Figure 6. The two H-bonds have different lengths, namely the H-bond involving one of the carboxylic oxygen atoms is at 1.897 Å, whilst that involving the glycosidic oxygen atom is at 2.207 Å, respectively.

A close inspection at the frontier orbitals of the dimer reveals that the HOMO is localized on the Arg97 fragment whereas the LUMO is localized on both the carboxylic and glycosidic NeuNAc moieties. This result agrees

with that obtained for the LUMO level of sLe^X depicted in Figure 5d. The BSSE-corrected binding energy calculated for the H-bonded dimer corresponds to 16.63 kcal/mol. This quantity contributes, together with those of other interactions, to the total free energy of binding of the E-selectin/sLe^X complex. To the best of our knowledge, this thermodynamic quantity has not been measured yet.

Electrostatic potential

Electrostatic complementary between protein and ligand surfaces is likely to drive a variety of molecular recognition processes.[22] The electrostatic potential (ESP) is determined by the magnitude of the atomic charges which, in the present study, were derived from a Mulliken population analysis[23] of the RHF-AM1/COSMO wavefunction. Figure 7 displays the ESP surfaces of the anionic and neutral forms of bioactive conformer **A**. The ESP surface of the anion, shown on the left side of Figure 7, displays a prominent negative potential character (colored in blue), with a small spot of positive potential (colored in red) located between the Fuc moiety and the NHAc residue of Glc.

On the other hand, the ESP surface of the neutral (i.e., protonated) sugar, shown on the right side of Figure 7, reveals a uniform distribution of positive and negative area. Hence, its global character is essentially neutral. This feature qualitatively agrees with the observations of Somers et al.,[5] according to which the sLe^X component of the SGP-3 ligand interacts with P-selectin in an area of neutral or negative ESP.[24] Furthermore, we notice that the Fuc moiety generates both positive and negative ESP surface areas. This feature might account for the differences in binding between sLe^X and the Ca^{2+} ions bound on the CRDs of selectins and the MBP mutant, respectively.

Conformational flexibility of the NeuNAc residue

As already mentioned, rotations about the C–O–C bonds of the αNeuNAc(2-3)βGal glycosidic linkage give rise to three canonical conformations, which have been labeled **A**, **B**, and **C**, respectively. The remaining part of the sLe^X molecule, however, appears to be relatively stereorigid.[16] A possible explanation for such a conformational behavior might be related to the electron density distribution within sLe^X itself. In this regard, an inspection of the Mulliken atomic charges calculated for the neutral sugar reveals that, in addition to the negative charges born by the oxygen atoms, negative charge is concentrated on the terminal NHAc moieties of both GlcNAc and NeuNAc. Hence, intramolecular Coulomb-type repulsive interactions might be at the origin of the low conformational freedom of the $Lewis^X$ portion of the sLe^X molecule.

Comparing the optimized torsional parameters of conformer **A** with the corresponding experimental values given at the bottom of Table 2 is not sufficient to establish what protonation state is being adopted by the bounded sugar. Hence, we need to assess the conformational flexibility about the αNeuNAc(2-3)βGal glycosidic linkage of sLe^X in both the anionic and neutral states. For this purpose we performed a series of

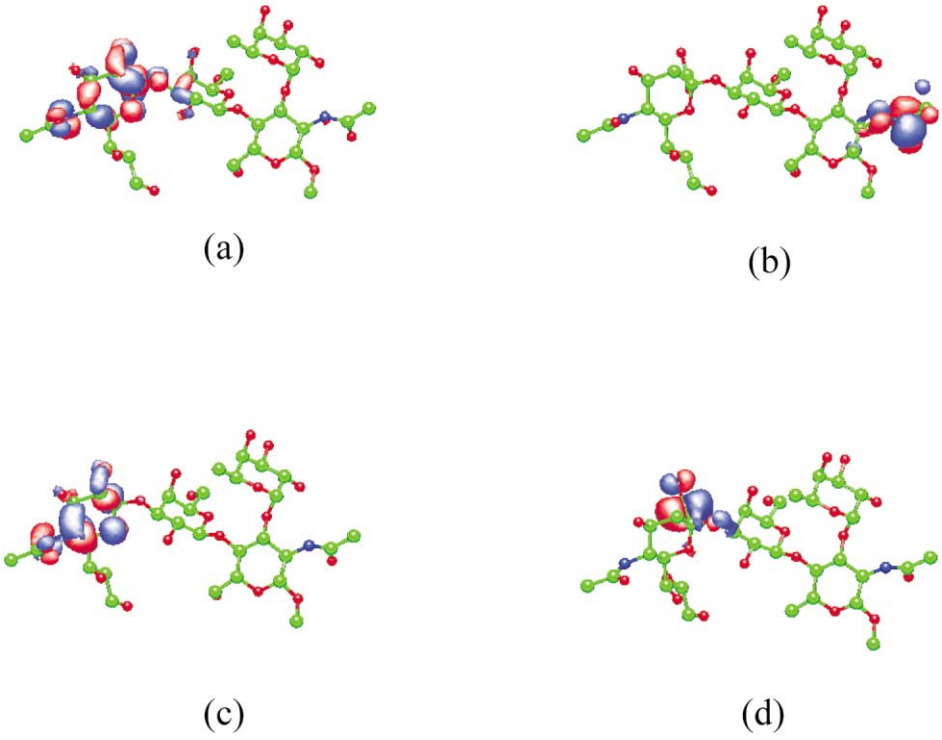

Figure 5. Frontier molecular orbitals of sLe^X (conformer **A**) in the (a,b) anionic and (c,d) neutral states: (a,c) HOMO and (b,d) LUMO levels. AM1/COSMO results. In each drawing, the NeuNAc residue is on the left side and GlcNAc on the right side. Hydrogen atoms have been omitted for clarity.

relaxed potential energy surface scans in which the torsion angles ϕ_1 and ψ_1 were varied in steps of 36°, starting from the optimized geometry of conformer **A** (see Table 2), while the remaining degrees of freedom were fully relaxed. A total of one hundred conformations were sampled for each state and the corresponding HOF, calculated with the AM1/COSMO method, are plotted in Figure 8. The data in both graphs were fitted with a moving average function of period two. The first point on the left side plot of Figure 8 corresponds to the HOF of conformer **A** in the anionic state (Table 2). Although the latter corresponds to a local minimum energy structure, there exist several other conformers which are more stable than that. The 13th conformer, with torsion angles at 133.7 and −54.8°, is that with the lowest-energy whereas the 27th conformer, with torsion angles at 169.7 and 90.8°, is characterized by the highest energy content. The latter conformer is separated from **A** by an energy barrier of about 35 kcal/mol, which originates from a repulsive steric interaction between the hydrogen atoms at C2 on NeuNAc and the OH group at C4 on Gal.

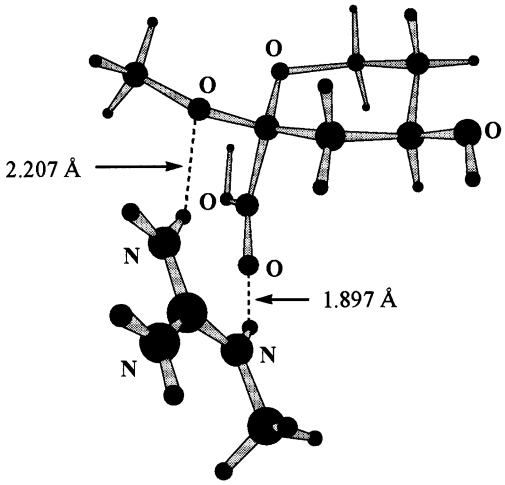

Figure 6. Optimized structure of the H-bonded dimer representing a minimal model of the NeuNAc/Arg97 interaction. The structure was geometry optimized at the RHF/6–31G(d,p) level of theory with the GAMESS package. Only the heteroatoms are labeled.

The graph on the right side of Figure 8, corresponding to the distribution of the HOF for the neutral sLe^X conformers, is somewhat different from that described above. Here, the 85th conformer, with torsion angles at 25.7 and 233.2°, is that with the highest energy content and, most important, conformer **A** is now amongst the low-energy conformers. It must be noted, however, that the bioactive conformer is not the one with the lowest energy. In this regard, Janssen[25] has recently shown that higher energy conformations have a higher affinity for

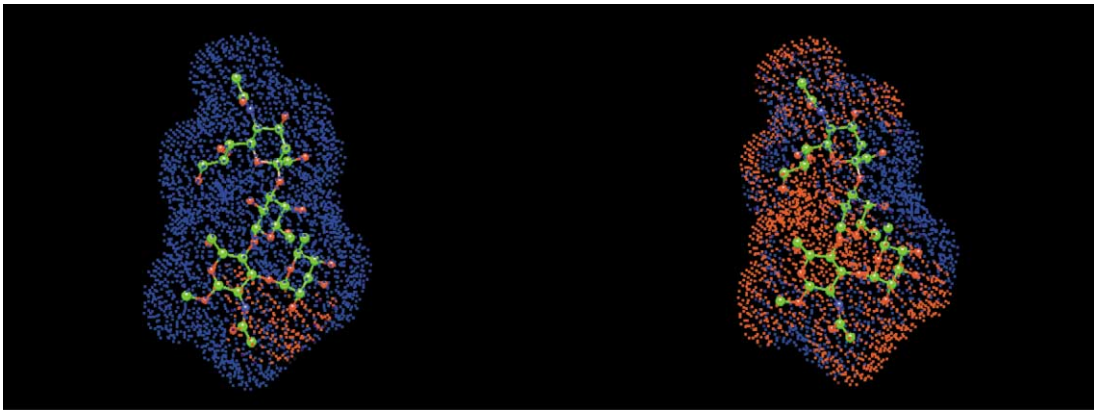

Figure 7. Electrostatic potential surfaces of sLe^X (conformer **A**) in the anionic (left side) and neutral (right side) state as calculated with the AM1/COSMO method. Red and blue colors correspond to positive and negative potential, respectively. The NeuNAc residue is located on the top of each drawing. Hydrogen atoms have been omitted for clarity.

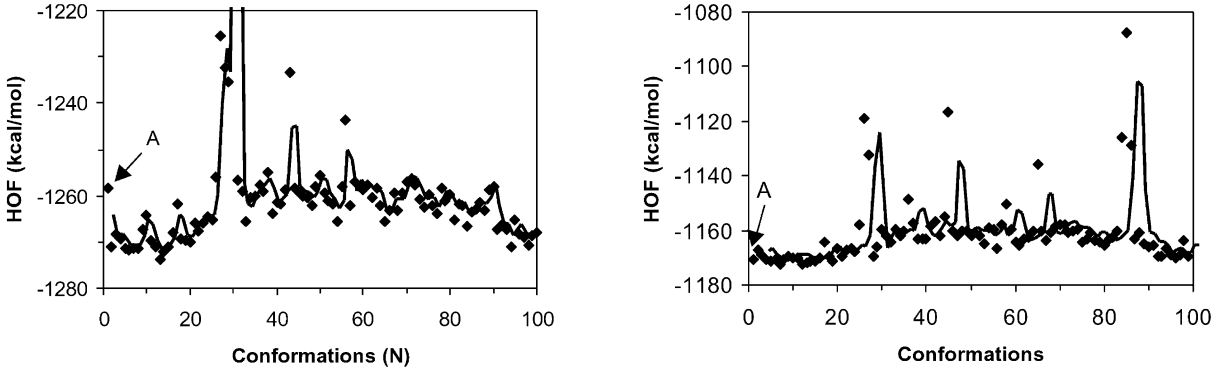

Figure 8. Distribution of the heats of formation (HOF) of sLe^X in the anionic (left side) and neutral (right side) states for rotations about the torsion angles ϕ_1 and ψ_1 by incremental steps of 36°. The data in both graphs were fitted with a moving average function of period two.

the receptor than lower energy conformations. The HOF calculated with the AM1/COSMO method (Table 1) along with solution NMR studies[16] seem to support this view.

Conclusion

The results of our quantum chemical calculations on the sLe^X molecule strongly suggest that the sugar in its bioactive conformation binds the CRD of E-selectin in the neutral (i.e., protonated) state rather than in the anionic one. This finding nicely agrees with the pattern of the atom–atom contacts thus far revealed by the 3-D structure of the E-selectin/sLe^X complex, which has been recently characterized by X-ray diffraction crystallography.[5] We expect the present results to have interesting implications for the design of new sLe^X mimics.

Methods

All the semi-empirical MO calculations were performed with the MOPAC2000® (Version 1.33) software package.[26] The structures of different sLe^X conformers were fully optimized at the restricted Hartree–Fock (RHF) level by employing both the AM1[27] and PM3[28] semi-empirical hamiltonians. The geometry optimizations were performed by including the effect of an acqueous medium with the aid of the Conductor-like Screening Model (COSMO) of Klamt and Schürmann.[29] COSMO is a continuum solvation model in which the effect of the solvent is simulated by introducing an ε-dependent correction factor into either the AM1 or PM3 energy hamiltonians ($\varepsilon = 78.5$ for water at 25 °C). This method has produced excellent results for the solvation energies of medium and large size molecules and is expected to perform well for sugars as well.

The eigenvector-following routine of Baker[30] was employed in all the gradient minimizations, with the default termination criteria increased by a factor of 100. A molecular mechanics correction was applied to each peptide bond (of NHAc) optimized with the PM3 method. This increases the barrier to rotation about the peptide bond by ca. 14 kcal/mol thus preventing the pyramidalization of the sp^2 nitrogen atom.[26] This type of problem is not encountered with the AM1 method. Potential energy surface scans about selected pairs of torsion angles were performed with the grid algorithm provided by MOPAC2000®.[26]

The ab initio MO calculations were performed with the GAMESS code.[31] For this purpose, the structure of a model dimer was optimized with the RHF method[32] by employing the 6-31G(d,p) basis set of Pople and co-workers.[33] The resulting binding energy was corrected for the basis set superposition error (BSSE) by employing the counterpoise correction method.[32] The WinMOPAC® (version 3.0),[34] Molden (version 3.6),[35] and Tornado (version 0.48)[36] graphic packages were employed for all the pre- and post-processing operations.

Acknowledgements

The authors are grateful to Dr. J. J. P. Stewart (Stewart Computational Chemistry) for his precious technical advice on the MOPAC2000® package and to S. Sakai for help with Tornado.

References and Notes

1. Varki, A. *Proc. Natl. Acad. Sci. U.S.A.* **1994**, *91*, 7390.
2. Lasky, L. A. *Ann. Rev. Biochem.* **1995**, *64*, 113.
3. Simanek, E. E.; McGarvey, G. J.; Jablonovski, J. A.; Wong, C.-H. *Chem. Rev.* **1998**, *98*, 833.
4. Weis, W. I.; Drickhamer, K. *Ann. Rev. Biochem.* **1996**, *65*, 441.
5. Somers, W. S.; Tang, J.; Shaw, G. D.; Camphausen, R. T. *Cell* **2000**, *103*, 467.
6. Graves, B. J.; Crowther, R. L.; Chandran, C.; Rumberger, J. M.; Li, S.; Huang, K.-S.; Presky, D. H.; Familletti, P. C.; Wolitzky, B. A.; Burns, D. K. *Nature* **1994**, *367*, 4431.
7. Drenth, J. *Principles of Protein X-Ray Crystallography*, 2nd ed.; Springer: Berlin, 1999.
8. Thiel, W. *Adv. Chem. Phys.* **1996**, *93*, 703.
9. Stewart, J. J. P. *Int. J. Quantum Chem.* **1996**, *58*, 133.
10. Stewart, J. J. P. *J. Mol. Struct. (Theochem)* **1997**, *401*, 195.
11. Pichierri, F.; Sarai, A. *Chem. Phys. Lett.* **2000**, *322*, 536.
12. Cramer, C. J.; Truhlar, D. G. *Chem. Rev.* **1999**, *99*, 2161.
13. Rappe, A. K.; Casewit, C. J. *Molecular Mechanics Across Chemistry*; University Science: Sausalito, 1997.
14. Ng, K. K.-S.; Weis, W. I. *Biochemistry* **1997**, *36*, 980.
15. Berman, H. M.; Westbrook, J.; Feng, Z.; Gilliland, G.; Bhat, T. N.; Weissig, H.; Shindyalov, I. N.; Bourne, P. E. *Nucl. Acids Res.* **2000**, *28*, 235.
16. Imberty, A.; Péres, S. *Chem. Rev.* **2000**, *100*, 4567.
17. Mukhopadhyay, C.; Miller, K. E.; Bush, C. A. *Biopolymers* **1994**, *34*, 21.
18. Kirschener, K. N.; Lee, M.; Stanley, R. C.; Bowen, J. P. *Bioorg. Med. Chem.* **2000**, *8*, 329.
19. Porschke, D. *Biophys. Chem.* **1997**, *66*, 241.
20. Fukui, K. *Angew. Chem., Int. Ed. Engl.* **1982**, *21*, 801.
21. Albright, T. A.; Burdett, J. K.; Whangbo, M.-H. *Orbital Interactions in Chemistry*; John Wiley and Sons: New York, 1985.
22. Nakamura, H. *Quart. Rev. Biophys.* **1996**, *29*, 1.
23. Mulliken, R. S. *J. Chem. Phys.* **1955**, *23*, 1833.
24. It is worth noticing that the graphical representation of the ESP surface derived from Poisson–Boltzman calculations adopts an opposite coloring convention from the one adopted here.
25. Janssen, L. H. M. *Bioorg. Med. Chem.* **1998**, *6*, 785.
26. Stewart, J. J. P. *MOPAC2000® Manual*; Fujitsu Ltd: Tokyo, 1999.
27. Dewar, M. J. S.; Zoebish, E. G.; Healy, E. F.; Stewart, J. J. P. *J. Am. Chem. Soc.* **1985**, *107*, 3902.
28. Stewart, J. J. P. *J. Comput. Chem.* **1989**, *10*, 209.
29. Klamt, A.; Schürmann, G. *J. Chem. Soc., Perkin Trans. 2* **1993**, 799.
30. Baker, J. *J. Comput. Chem.* **1986**, *7*, 385.
31. Schmidt, M. W.; Baldridge, K. K.; Boatz, J. A.; Elbert, S. T.; Gordon, M. S.; Jensen, J. H.; Koseki, S.; Matsunaga, N.; Nguyen, K. A.; Su, S. J.; Windus, T. L.; Dupuis, M.; Montgomery, J. A. *J. Comp. Chem.* **1993**, *14*, 1347.
32. Jensen, F. *Introduction to Computational Chemistry*; John Wiley and Sons: Chichester, 1999.
33. Hariharan, P. C.; Pople, J. A. *Mol. Phys.* **1974**, *27*, 209.
34. *WinMOPAC®*, version 3.0; Fujitsu Ltd.: Tokyo.
35. Shaftenaar, G.; Noordik, J. H. *J. Comput.-Aided Mol. Des.* **2000**, *14*, 123.
36. Sakai, S. *Tornado*, version 0.48; RIKEN Genomic Sciences Center: Yokohama.